

# Donepezil blocks voltage-gated ion channels in rat dissociated hippocampal neurons

Bo Yu, Guo-Yuan Hu\*

State Key Laboratory of Drug Research, Shanghai Institute of Materia Medica, Shanghai Institutes for Biological Sciences,  
Chinese Academy of Sciences, Shanghai 201203, PR China

Received 17 July 2004; received in revised form 29 November 2004; accepted 6 December 2004

Available online 7 January 2005

## Abstract

Donepezil (E2020) is a novel cholinesterase inhibitor for the treatment of Alzheimer's disease. Recent studies show that it may act on targets other than acetylcholinesterase in the brain. In the present study, the actions of donepezil on voltage-gated  $\text{Na}^+$  and  $\text{K}^+$  channels were investigated in rat dissociated hippocampal neurons. Donepezil reversibly inhibited voltage-activated  $\text{Na}^+$  current ( $I_{\text{Na}}$ ), delayed rectifier  $\text{K}^+$  current ( $I_{\text{K}}$ ) and fast transient  $\text{K}^+$  current ( $I_{\text{A}}$ ). The inhibition of donepezil on  $I_{\text{Na}}$  was dependent on the holding potential. When neurons were held at  $-100$ ,  $-80$  and  $-60$  mV, the  $\text{IC}_{50}$  value was  $436 \pm 19$ ,  $291 \pm 26$  and  $3.8 \pm 0.3$   $\mu\text{M}$ , respectively. The drug did not affect the activation, fast inactivation of  $I_{\text{Na}}$  and its recovery from fast inactivation. The inhibition of donepezil on  $I_{\text{K}}$  ( $\text{IC}_{50} = 78 \pm 5$   $\mu\text{M}$ ) was voltage-dependent, whereas that on  $I_{\text{A}}$  ( $\text{IC}_{50} = 249 \pm 25$   $\mu\text{M}$ ) was voltage-independent. Donepezil caused a significant hyperpolarizing shift of the voltage-dependence of the activation and steady-state inactivation of  $I_{\text{K}}$ , without affecting the kinetic properties of  $I_{\text{A}}$ . Due to the high concentrations used, the blocking effects of donepezil on the voltage-gated ion channels are unlikely to contribute to the clinical benefits in patients with Alzheimer's disease.

© 2004 Elsevier B.V. All rights reserved.

**Keywords:** Alzheimer's disease; Cholinesterase inhibitor; Donepezil (E2020);  $\text{Na}^+$  channel;  $\text{K}^+$  channel

## 1. Introduction

Alzheimer's disease affects more than 15 million people worldwide. As the proportion of elderly in the population accelerates rapidly, its incidence will steadily increase. However, the current situation in pharmacotherapy for the disease is unsatisfactory. Thus far, only cholinesterase inhibitors are available as the palliative drugs to ameliorate the cognitive deficits in mild to moderately severe Alzheimer's disease (Giacobini, 2000; Palmer, 2002). Accumulative evidence points out that the actions of cholinesterase inhibitors are not confined to inhibition of acetylcholinesterase in the brain. For example, most

cholinesterase inhibitors, such as tacrine, galantamine, rivastigmine and huperzine A, have been found to block voltage-gated  $\text{Na}^+$  and  $\text{K}^+$  channels in mammalian cortical neurons (Rogawski, 1987; Li and Hu, 2002a,b; Pan et al., 2003, 2004). It was proposed that inhibition of the delayed rectifier  $\text{K}^+$  current by low concentrations of tacrine or galantamine might be related to the clinical benefits in patients with Alzheimer's disease (Kraliz and Singh, 1997; Pan et al., 2003).

Donepezil (( $\pm$ )-2-[(1-benzylpiperidin-4-yl)methyl]-5,6-dimethoxy-indan-1-one monohydrochloride, E2020) is one of the second generation of cholinesterase inhibitors for the treatment of Alzheimer's disease. The drug was demonstrated to be a potent and selective inhibitor of brain acetylcholinesterase with less adverse effects than physostigmine and tacrine (Sugimoto et al., 2000). However, it is unknown whether donepezil resembles other cholinesterase inhibitors in blockade of voltage-

\* Corresponding author. Tel.: +86 21 5080 6778; fax: +86 21 5080 7088.

E-mail address: [gyhu@mail.shcnc.ac.cn](mailto:gyhu@mail.shcnc.ac.cn) (G.-Y. Hu).

gated  $\text{Na}^+$  channels and/or  $\text{K}^+$  channels in the brain, although an inhibitory effect on the delayed rectifier-like  $\text{K}^+$  current has been noted (Zhong et al., 2002). To clarify the question, we investigated the actions of donepezil on voltage-gated ion channels in rat dissociated hippocampal CA1 pyramidal neurons using whole-cell voltage-clamp technique.

## 2. Materials and methods

### 2.1. Reagents

Donepezil and huperzine A were colorless crystals (purity >98%) provided by the Department of Medicinal Chemistry and the Department of Phytochemistry of

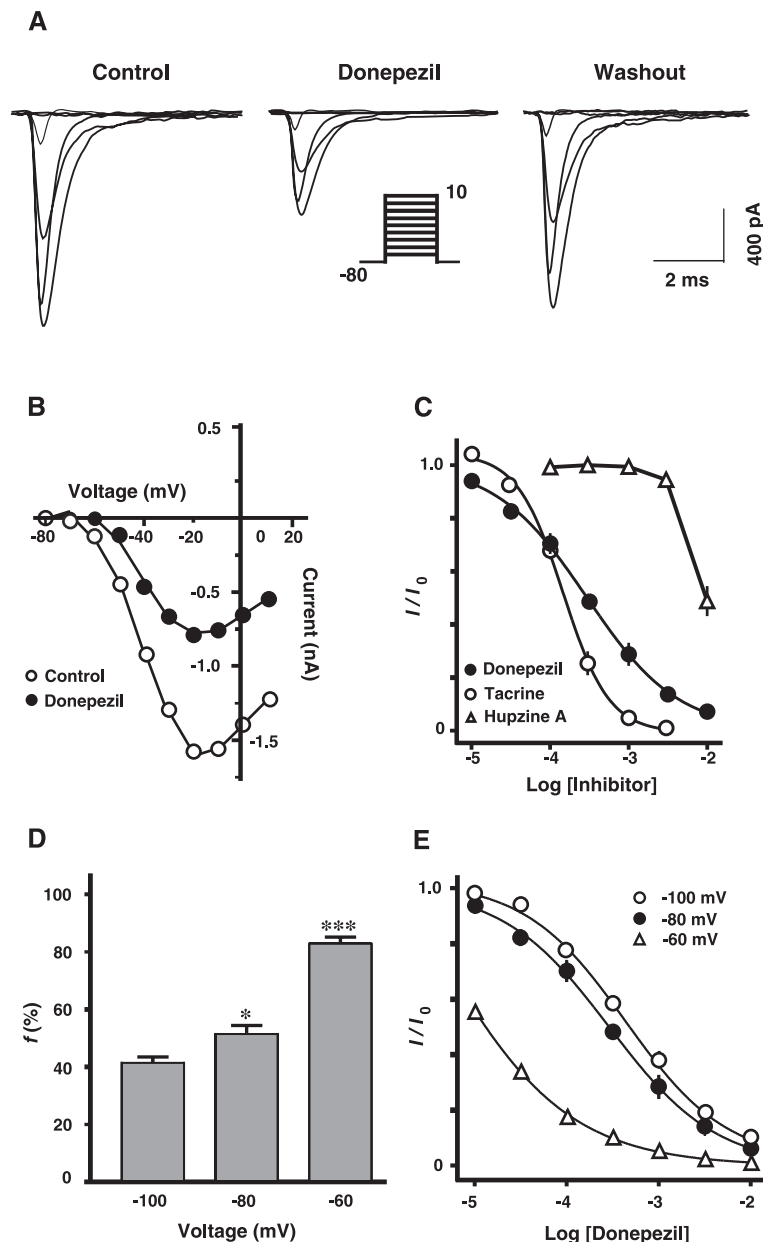


Fig. 1. Inhibitory effect of donepezil on voltage-activated  $\text{Na}^+$  current in rat hippocampal neurons. (A) The representative  $\text{Na}^+$  current traces before (left), during application of  $300 \mu\text{M}$  donepezil (middle) and after washout of the drug for 1 min (right). The neuron was held at  $-80 \text{ mV}$  and currents were elicited with a series of 20-ms depolarizing steps (from  $-70 \text{ mV}$  to  $+10 \text{ mV}$ , with  $10 \text{ mV}$  increment), then back to  $-80 \text{ mV}$ , delivered every 10 s (the inset). For clarity, only the traces elicited in steps to  $-70$ ,  $-60$ ,  $-40$ ,  $-20$  and  $0 \text{ mV}$  are shown. (B) Current–voltage ( $I/V$ ) curves before and during application of  $300 \mu\text{M}$  donepezil from the same neuron in (A). (C) Concentration–inhibition curves of donepezil, tacrine and huperzine A ( $n=6$  for each). Neurons were held at  $-80 \text{ mV}$  and currents were elicited in steps to  $-20 \text{ mV}$ . (D) Fractional inhibition of  $\text{Na}^+$  current by  $300 \mu\text{M}$  donepezil at the holding potential of  $-100$ ,  $-80$  and  $-60 \text{ mV}$ . Currents were elicited in steps to  $-20 \text{ mV}$ . Each column is mean  $\pm$  S.E.M. ( $n=6-7$ ).  $*P<0.05$ ,  $***P<0.001$  versus the  $f$  value at the holding potential of  $-100 \text{ mV}$  (Student's unpaired  $t$ -test). (E) Concentration–inhibition curves of donepezil at the holding potential of  $-100$ ,  $-80$  and  $-60 \text{ mV}$  ( $n=6-7$ ). Currents were elicited in steps to  $-20 \text{ mV}$ . In (C) and (E), more than a half of symbols have error bars smaller than their size. The smooth lines are the fit curves.

Shanghai Institute of Materia Medica. Other chemicals were purchased from Sigma (St. Louis, MO, USA).

## 2.2. Preparation of dissociated hippocampal neurons

All procedures were performed in accordance with the institutional guidelines on the care and use of experimental animals set by the Chinese Academy of Sciences. Dissociated CA1 pyramidal neurons were prepared from 2- to 5-day-old Sprague–Dawley rats as previously described (Li and Hu, 2002a). Briefly, transverse minislices (500  $\mu\text{m}$ ) of the hippocampal CA1 region were cut in an oxygenated ice-cold dissociation solution. The dissociation solution consisted of (in mM):  $\text{Na}_2\text{SO}_4$  82,  $\text{K}_2\text{SO}_4$  30,  $\text{MgCl}_2$  5, HEPES 10 and glucose 10 at pH 7.4 with NaOH. The slices were incubated in dissociation solution containing protease XXIII (3 mg/ml) at 32 °C for 8 min, and then placed in dissociation solution containing trypsin inhibitor type II-S (1 mg/ml) and bovine serum albumin (1 mg/ml) at room temperature under an oxygen atmosphere until use. The slices remained viable at least for 5–6 h.

When neurons were needed, two to three pieces of slice were triturated using a series of fire-polished Pasteur pipettes with decreasing tip diameters. The neurons were placed in a recording dish and perfused with an external solution.

## 2.3. Whole-cell voltage-clamp recording

The recording was made from pyramidal-shaped neurons (capacitance 4–10 pF) using an Axopatch 200 A amplifier (Axon Instruments, USA) at 21–23 °C. The electrodes (tip resistance 3–4 M $\Omega$ ) were pulled from borosilicate glass pipettes (Hilgenberg, Germany) and filled with an internal solution. The voltage-activated currents were elicited by command protocols provided by pClamp 9.0 software via a DigiData-1322 A interface (Axon Instruments, USA). Series resistance was compensated by 75–85% to minimize the remaining voltage error less than 5 mV. The liquid junction potential measured to be less than 3 mV was not compensated. Linear leak and residual capacitance currents were subtracted on-line using a P/–4 protocol. Signals were

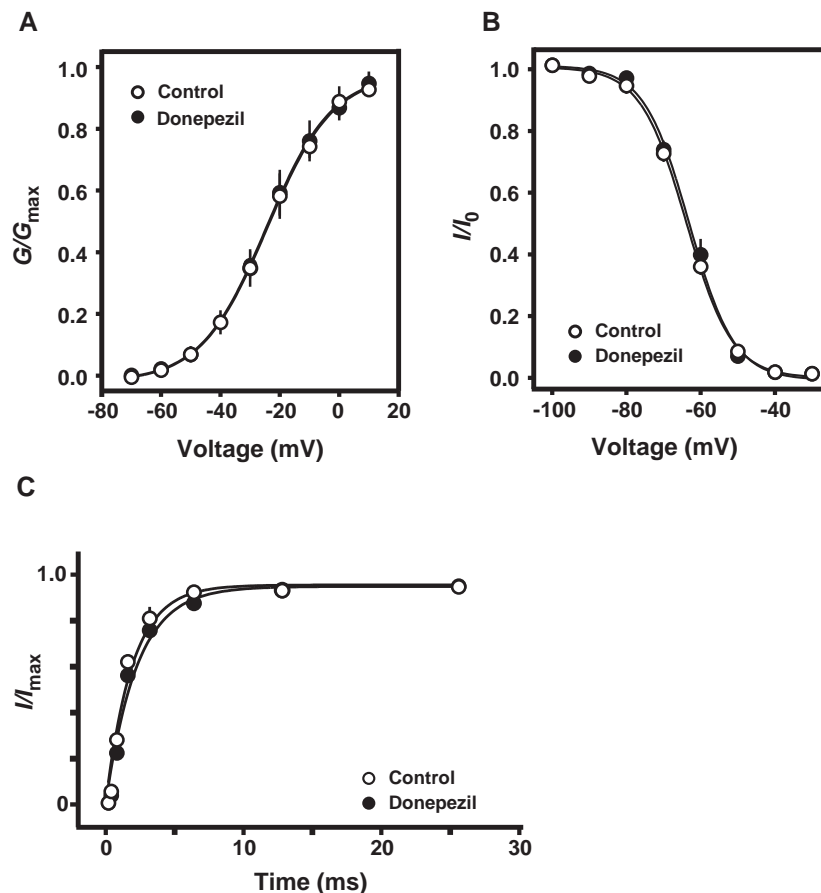


Fig. 2. Effect of donepezil on kinetic properties of voltage-activated  $\text{Na}^+$  current. (A), (B) and (C) show the activation curves, fast inactivation curves and the time courses of recovery from fast inactivation, respectively, in control and in the presence of 300  $\mu\text{M}$  donepezil. Some symbols have error bars smaller than their size. Neurons were held at  $-80$  mV. Three different protocols were used, but all delivered every 10 s. For studying activation: 20-ms depolarizing steps from  $-70$  mV to  $+10$  mV with 10 mV increment, then back to  $-80$  mV ( $n=6$ ). For studying fast inactivation: 100-ms prepulses at different potentials ( $-100$  mV to  $-30$  mV with 10 mV increment) were followed by a 20-ms step to  $-20$  mV, then back to  $-80$  mV ( $n=5$ ). For studying the recovery from fast inactivation: intervals of varying duration (0.2 to 25.6 ms) at  $-110$  mV were inserted between a 20-ms prepulse to  $-20$  mV and a 20-ms step to  $-20$  mV ( $n=7$ ).

filtered at 5 kHz, sampled at frequencies of 20 kHz and stored in an IBM-compatible computer.

#### 2.4. Solutions and drug application

For studying  $\text{Na}^+$  channel, the external solution contained (in mM): NaCl 120, TEA-Cl 20, KCl 5,  $\text{CaCl}_2$  1,  $\text{MgCl}_2$  1.25, HEPES 10 and glucose 10 at pH 7.4 with NaOH; the internal solution consisted of (in mM): CsCl 130, NaCl 10,  $\text{MgCl}_2$  1,  $\text{CaCl}_2$  1, HEPES 10 and EGTA 10 at pH 7.4 with CsOH. For studying  $\text{K}^+$  channels, the external solution contained (in mM): NaCl 135, KCl 5,  $\text{CaCl}_2$  1,  $\text{MgCl}_2$  2, HEPES 10, glucose 10 and tetrodotoxin 0.001 at pH 7.4 with NaOH; the internal solution had the following composition (in mM): potassium gluconate 125, KCl 20,  $\text{MgCl}_2$  2,  $\text{CaCl}_2$  1, HEPES 10 and EGTA 10 at pH 7.4 with KOH.

Cholinesterase inhibitors were dissolved in the external solutions. The pH and osmolality of drug-containing solutions were readjusted. The solutions were directly applied to the recorded neuron using RSC-100 Rapid Solution Changer with a nine-tube head (BioLogic France).

#### 2.5. Data analysis

The peak amplitude of  $I_{\text{Na}}$  and  $I_{\text{A}}$  was measured. The amplitude of  $I_{\text{K}}$  was measured with a 300-ms latency. The  $\text{IC}_{50}$  values for cholinesterase inhibitors in inhibition of voltage-activated current were determined using the equation:

$I/I_0 = 1/\{1 + [C/\text{IC}_{50}]^n\}$ , where  $I_0$  and  $I$  are the current amplitude in control and in the presence of a cholinesterase inhibitor,  $C$  is the concentrations of the inhibitor in the external solution and  $n$  is the Hill coefficient. The fractional inhibition ( $f$ ) by donepezil was calculated with the equation:  $f = (1 - I/I_0) \cdot 100\%$ , where  $I_0$  and  $I$  are the current amplitude in control and in the presence of a given concentration of donepezil. Activation and inactivation plots were fitted to the Boltzmann equation:  $Y = 1/\{1 + \exp[(V - V_{1/2})/k]\}$ , where  $Y$  is the normalized conductance or current,  $V$  is the membrane potential,  $V_{1/2}$  is the voltage at half-maximal activation or inactivation and  $k$  is the slope factor. The time course of recovery from inactivation was fitted with a single exponential function. Data are presented as mean  $\pm$  S.E.M. Student's paired or unpaired two-tailed  $t$ -test was used for statistical analysis.

### 3. Results

#### 3.1. Inhibitory effect of donepezil on voltage-activated sodium current in hippocampal neurons

Application of donepezil at the concentrations above 10  $\mu\text{M}$  caused marked reduction in the peak amplitude of fast voltage-activated  $\text{Na}^+$  current ( $I_{\text{Na}}$ ) elicited from a holding potential of  $-80$  mV (Fig. 1A,B). This effect was reversible and concentration-dependent ( $\text{IC}_{50} = 291 \pm 26$   $\mu\text{M}$ , Hill coef-

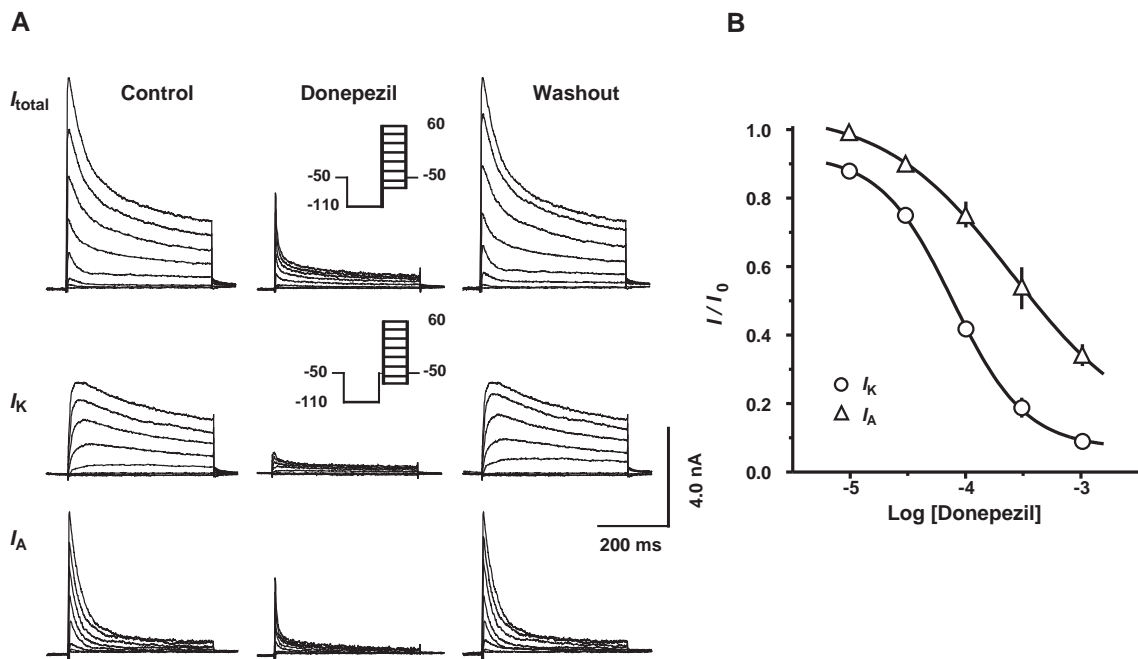


Fig. 3. Inhibitory effect of donepezil on voltage-activated  $\text{K}^+$  currents in rat hippocampal neurons. (A) The upper, middle and lower traces are the representative current families for the total  $\text{K}^+$  currents ( $I_{\text{total}}$ ), delayed rectifier  $\text{K}^+$  currents ( $I_{\text{K}}$ ) and fast transient  $\text{K}^+$  currents ( $I_{\text{A}}$ ), respectively, before, during application of 300  $\mu\text{M}$  donepezil and after washout of the drug for 1 min. The neuron was held at  $-50$  mV. To elicit  $I_{\text{total}}$ : a 600-ms hyperpolarizing prepulse to  $-110$  mV was followed by a series of 400-ms steps from  $-80$  mV to  $+60$  mV with 10 mV increment, delivered every 10 s (the upper inset). To elicit  $I_{\text{K}}$ , a similar protocol, but a 50-ms interval at  $-50$  mV was inserted after the prepulse (the middle inset).  $I_{\text{A}}$  is the subtraction of  $I_{\text{K}}$  from  $I_{\text{total}}$ . (B) Concentration-inhibition curves of donepezil in inhibition of voltage-activated  $\text{K}^+$  currents ( $n=6$  for each curve). Currents were elicited in steps to  $+40$  mV. More than a half of symbols have error bars smaller than their size. The smooth lines are the fit curves.

ficient =  $0.7 \pm 0.2$ ,  $n=6$ ) (Fig. 1C). For comparison, the effect of two other cholinesterase inhibitors on  $I_{Na}$  was examined at the same holding potential of  $-80$  mV: tacrine is almost twice more potent than donepezil ( $IC_{50} = 158 \pm 34$   $\mu$ M, Hill coefficient =  $1.67 \pm 0.51$ ,  $n=6$ ), whereas huperzine A at 10 mM caused a reduction of  $55.6 \pm 8.8\%$  ( $n=6$ ) in the peak amplitude of  $I_{Na}$ .

The inhibitory effect of donepezil on  $I_{Na}$  was dependent on the holding potential: it became more prominent when neurons were held at more depolarizing membrane potentials. The fractional inhibition by 300  $\mu$ M donepezil was  $41.7 \pm 1.7\%$  at the holding potential of  $-100$  mV,  $51.8 \pm 2.6\%$  at  $-80$  mV and  $83.0 \pm 2.2\%$  at  $-60$  mV ( $n=6-7$ ; Fig. 1D). The  $f$  values at the holding potential of  $-80$  and  $-60$  mV were significantly different from that at  $-100$  mV. The  $IC_{50}$  value of donepezil was also changed with the holding potential. The  $IC_{50}$  value at the three holding potentials was  $436 \pm 19$   $\mu$ M ( $n=6$ ),  $291 \pm 26$   $\mu$ M ( $n=6$ ) and  $3.8 \pm 0.3$   $\mu$ M ( $n=7$ ), respectively (Fig. 1E).

### 3.2. Effect of donepezil on kinetic properties of voltage-activated sodium current in hippocampal neurons

Application of donepezil did not affect the activation and fast inactivation of  $I_{Na}$ , as well as its recovery from fast inactivation (Fig. 2). In the presence of 300  $\mu$ M donepezil: the voltage for half-maximal activation was  $-24.6 \pm 1.1$  mV (versus  $-24.2 \pm 1.5$  mV in control,  $n=6$ ,  $P>0.05$ ); the voltage for half-maximal fast inactivation was  $-63.1 \pm 0.6$  mV (versus  $-63.9 \pm 0.5$  mV in control,  $n=5$ ,  $P>0.05$ ); the time constant of recovery from fast inactivation was  $2.3 \pm 0.2$  ms (versus  $1.9 \pm 0.2$  ms in control,  $n=7$ ,  $P>0.05$ ).

### 3.3. Inhibitory effect of donepezil on voltage-activated potassium currents in hippocampal neurons

Both the delayed rectifier  $K^+$  current ( $I_K$ ) and fast transient  $K^+$  current ( $I_A$ ) could be recorded from the same neuron by using the protocols shown in Fig. 3A and a subtraction procedure (Klee et al., 1995; Li and Hu, 2002a). Donepezil at the concentrations above 10  $\mu$ M reversibly inhibited both  $I_K$  and  $I_A$  at all depolarizing steps (Fig. 3A). The potency of donepezil in inhibition of  $I_K$  was nearly three-fold higher than that in inhibition of  $I_A$  (Fig. 3B). The  $IC_{50}$  value for inhibition of  $I_K$  and  $I_A$  was  $78 \pm 5$   $\mu$ M (Hill coefficient =  $1.4 \pm 0.2$ ,  $n=6$ ) and  $249 \pm 25$   $\mu$ M (Hill coefficient =  $0.9 \pm 0.4$ ,  $n=6$ ), respectively.

The inhibitory effect of donepezil on  $I_K$  was voltage-dependent. Application of donepezil caused an inward rectification of the current-voltage ( $I/V$ ) curve of  $I_K$  (Fig. 4A). As the neuron was stepped to more depolarizing membrane potentials, the inhibitory effect of donepezil was increased progressively. The fractional inhibition of  $I_K$  by 100  $\mu$ M donepezil tested in 5 neurons was  $58.3 \pm 2.7\%$  in step to 0 mV,  $65.9 \pm 3.2\%$  in step to +20 mV,  $68.9 \pm 3.0\%$  in step to +40 mV and  $71.8 \pm 2.2\%$  in step to

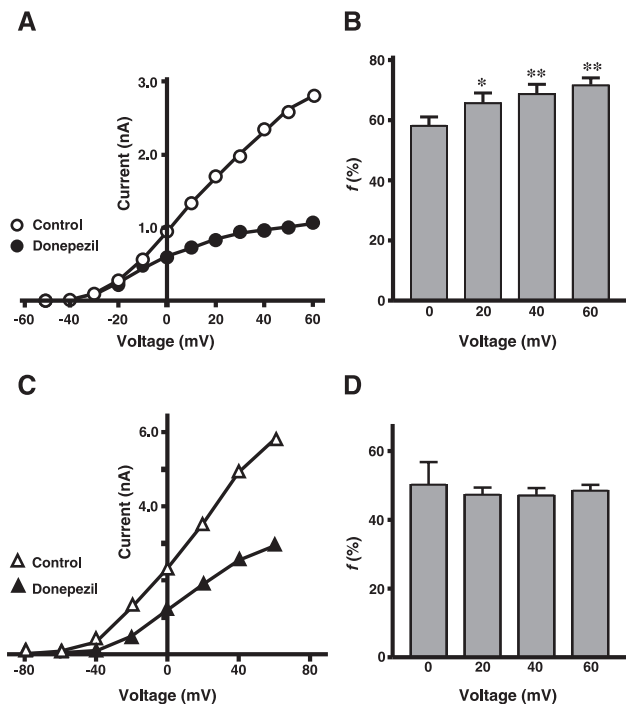


Fig. 4. Voltage-dependence of the inhibition by donepezil of the delayed rectifier  $K^+$  current. (A) Current-voltage ( $I/V$ ) curves of the delayed rectifier  $K^+$  current ( $I_K$ ) from a representative neuron before and during application of 100  $\mu$ M donepezil. (B) Fractional inhibition by 100  $\mu$ M donepezil of  $I_K$  elicited in step to 0, +20, +40 and +60 mV. Each column is mean  $\pm$  S.E.M. ( $n=5$ ). \* $P<0.05$ , \*\* $P<0.01$  versus the  $f$  value in step to 0 mV (Student's paired  $t$ -test). (C) Current-voltage ( $I/V$ ) curves of the fast transient  $K^+$  current ( $I_A$ ) from a representative neuron before and during application of 300  $\mu$ M donepezil. (D) Fractional inhibition by 300  $\mu$ M donepezil of  $I_A$  elicited in step to 0, +20, +40 and +60 mV. Each column is mean  $\pm$  S.E.M. ( $n=6$ ).

+60 mV (Fig. 4B). The  $f$  values in step to +20, +40 and +60 mV were significantly higher than that in step to 0 mV. In contrast, the inhibitory effect of donepezil on  $I_A$  was voltage-independent. Application of 300  $\mu$ M donepezil caused an apparent linear downward shift of the  $I/V$  curve of  $I_A$  (Fig. 4C). When the neuron was stepped to more depolarizing membrane potentials, the inhibitory effect of donepezil remained a nearly constant level. The fractional inhibition of  $I_A$  by 300  $\mu$ M donepezil tested in six neurons was  $50.4 \pm 6.4\%$  in step to 0 mV,  $47.5 \pm 1.9\%$  in step to +20 mV,  $47.2 \pm 2.0\%$  in step to +40 mV and  $48.7 \pm 1.5\%$  in step to +60 mV (Fig. 4D). There was no significant difference between the  $f$  values.

### 3.4. Effect of donepezil on kinetic properties of voltage-activated potassium currents in hippocampal neurons

Application of 100  $\mu$ M donepezil caused a significant hyperpolarizing shift of the voltage-dependence of the activation and steady-state inactivation of  $I_K$  (Fig. 5A,B). The voltage for half-maximal activation was changed from  $-7.0 \pm 1.0$  mV to  $-22.8 \pm 1.5$  mV ( $n=5$ ,  $P<0.01$ ), whereas the voltage for half-maximal inactivation from  $-80.9 \pm 0.5$



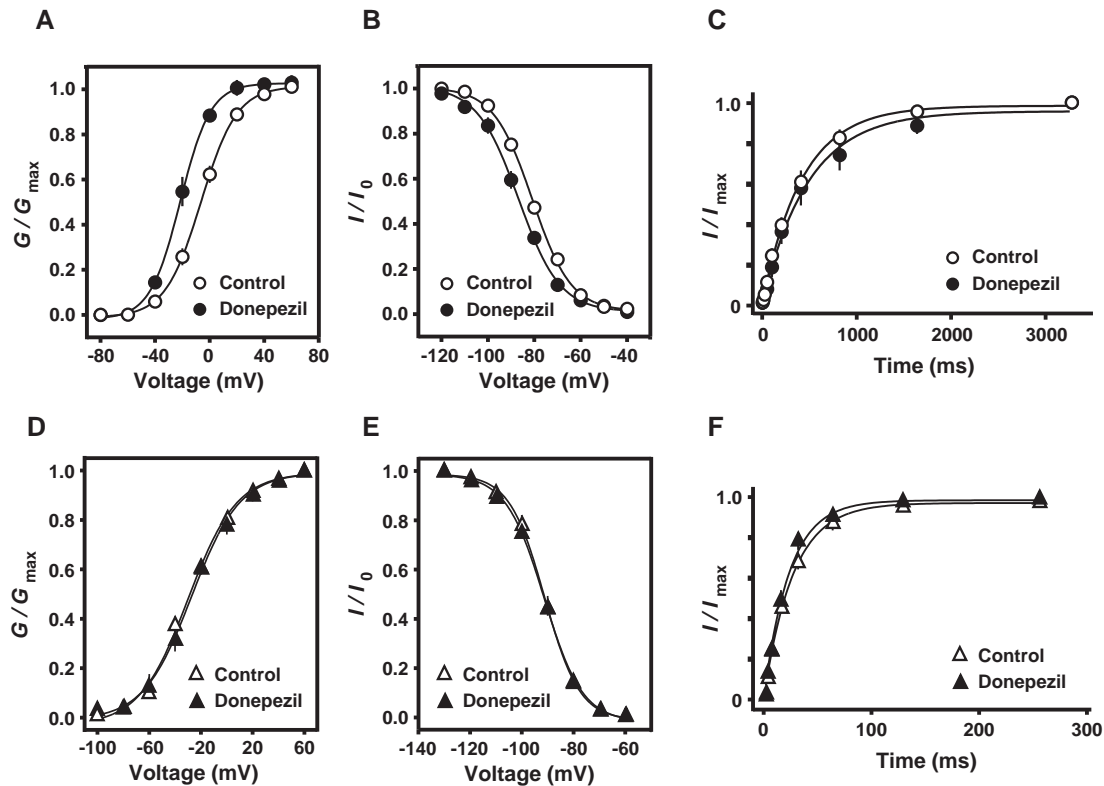


Fig. 5. Effect of donepezil on kinetic properties of voltage-activated  $K^+$  currents. (A), (B) and (C) are the activation curves and steady-state inactivation curves of the delayed rectifier  $K^+$  current ( $I_K$ ) and its time courses of recovery from steady-state inactivation, respectively, in control and in the presence of 100  $\mu$ M donepezil ( $n=5-6$ ). (D), (E) and (F) show a set of similar plots for the fast transient  $K^+$  current ( $I_A$ ), but tested with 300  $\mu$ M donepezil ( $n=6-7$ ). The protocols to study the activation are similar to those in Fig. 3A. For studying the steady-state inactivation, neurons were held at 0 mV, currents were elicited with a series of 600-ms prepulses at different hyperpolarizing potentials followed by a 400-ms step to +40 mV, then back to 0 mV, delivered every 10 s. For studying the time course of recovery from inactivation, neurons were held at 0 mV, currents were elicited on return from hyperpolarizing prepulses of varying durations at  $-110$  mV to 0 mV, delivered every 10 s. In each case,  $I_K$  was elicited using a protocol similar to that for  $I_A$ , but a 50-ms interval at  $-50$  mV was inserted after the prepulse.

mV to  $-86.8 \pm 0.9$  mV ( $n=5$ ,  $P < 0.01$ ). However, donepezil had no significant effect on the time course of recovery of  $I_K$  from inactivation (Fig. 5C). The time constant of recovery from inactivation was  $486.8 \pm 47.86$  ms in the presence of 100  $\mu$ M donepezil, (versus  $422.8 \pm 21.6$  ms in control,  $n=6$ ,  $P > 0.05$ ).

Donepezil did not change the kinetic properties of  $I_A$  (Fig. 5D–F). In the presence of 300  $\mu$ M donepezil, the voltage for half-maximal activation was  $-27.2 \pm 2.4$  mV (versus  $-30.0 \pm 1.5$  mV in control,  $n=6$ ,  $P > 0.05$ ); the voltage for half-maximal inactivation was  $-91.3 \pm 0.4$  mV (versus  $-91.2 \pm 0.7$  mV in control,  $n=7$ ,  $P > 0.05$ ); the time constant of recovery from inactivation was  $23.5 \pm 1.6$  ms (versus  $27.0 \pm 1.4$  ms in control,  $n=6$ ,  $P > 0.05$ ).

#### 4. Discussion

The present study demonstrates that donepezil at high concentrations reversibly blocks voltage-gated  $Na^+$  and  $K^+$  channels in rat hippocampal neurons. Therefore, there are striking resemblances in the pharmacological profile between donepezil and other cholinesterase inhibitors (Table

1). Recently, more pharmacological actions of donepezil have been addressed. For example, it was reported by Wang et al. (1999) that the drug exerted weak antagonism against *N*-methyl-D-aspartate (NMDA) receptor in rat cerebral cortex ( $IC_{50}=133.1$   $\mu$ M in [ $^3H$ ]MK-801 binding assay). Furthermore, donepezil was found to be effective to alleviate the oxygen-glucose deprivation-induced injury of PC12 cells (Zhou et al., 2001) and rat primary cultured

Table 1

Comparison of cholinesterase inhibitors in inhibition of acetylcholinesterase and voltage-activated ion currents in rat brain

	Acetylcholinesterase (nM)	$I_{Na}$ ( $\mu$ M)	$I_K$	$I_A$
<i>IC</i> <sub>50</sub> value of:				
Donepezil	$10.25 \pm 0.62^a$	$291 \pm 26^b$	$78 \pm 5$	$249 \pm 25$
Tacrine	$93.00 \pm 0.13^a$	$158 \pm 34^b$	$43 \pm 3^c$	$115 \pm 2^d$
Huperzine A	$66.58 \pm 0.51^a$	ND	$856 \pm 1^c$	$914 \pm 1^d$

All the values presented as mean  $\pm$  S.E.M. ND: could not be determined due to the low potency.

<sup>a</sup> Cheng et al. (1996).

<sup>b</sup> Measured at the holding potential of  $-80$  mV.

<sup>c</sup> Li and Hu (2002b).

<sup>d</sup> Li and Hu (2002a).

cortical neurons (Akasofu et al., 2003), as well as to protect rat primary cultured cortical neurons against glutamate-induced neurotoxicity (Takada et al., 2003). NMDA receptor plays an important role in acute hypoxic–ischemic injury and glutamate neurotoxicity in cortical neurons (Choi and Rothman, 1990). Because the concentration of donepezil to cause the neuroprotective effects ranged from 0.1 to 10  $\mu\text{M}$ , it seems to be impossible that the effects were mediated through antagonism against NMDA receptor. It has been demonstrated that selective blockade of voltage-gated  $\text{Na}^+$  channel by low concentrations of lidocaine or tetrodotoxin was effective in attenuation of the hypoxic damage in rat hippocampal slices (Raley-Susman et al., 2001). Although donepezil exerted a weak blocking effect on  $\text{Na}^+$  channel at more hyperpolarizing membrane potential ( $\text{IC}_{50}=291\pm 26$   $\mu\text{M}$  when neurons were held at  $-80$  mV), its potency greatly increased as the neurons were depolarized ( $\text{IC}_{50}=3.8\pm 0.3$   $\mu\text{M}$  at the holding potential of  $-60$  mV). It was found that hypoxia caused an initial small-amplitude hyperpolarization followed by a rapidly growing and marked depolarization in hippocampal pyramidal neurons (Raley-Susman et al., 2001). During the hypoxia-induced depolarization, donepezil 0.1 to 10  $\mu\text{M}$  might be sufficient to block the  $\text{Na}^+$  channel, thus to protect the neurons in vitro from hypoxic injury.

The relevance of block of ion channels by cholinesterase inhibitors to the treatment of Alzheimer's disease remains to be obscure. Thus far, there is few evidence to support such a link: Kraliz and Singh (1997) reported that tacrine at a concentration as low as 10  $\mu\text{M}$  was effective in inhibition of the delayed rectifier  $\text{K}^+$  current, and in broadening the action potentials in *Drosophila* larval muscles. Recently, Pan et al. (2003) found that 10  $\mu\text{M}$  galantamine markedly inhibited the delayed rectifier  $\text{K}^+$  current in rat hippocampal neurons. Because the concentrations were either within the plasma levels of tacrine measured in a clinical study, or close to the  $\text{IC}_{50}$  value of galantamine in inhibition of acetylcholinesterase, the authors proposed that blockade of the delayed rectifier  $\text{K}^+$  channels should prolong the duration of action potentials, leading to increasing the release of neurotransmitters into the synaptic cleft in the brain, thus contribute to the effectiveness in the treatment of Alzheimer's disease. In most cases, however, the potencies of cholinesterase inhibitors versus the ion channels are 3–4 orders of magnitude lower than on acetylcholinesterase (Table 1). During the treatment of Alzheimer's disease, the plasma concentration of cholinesterase inhibitors could probably never reach a level sufficient to block the voltage-gated ion channels in the brain. It was reported by Rogers et al. (1998) that the plasma concentration of donepezil in the patients receiving effective doses 5 or 10 mg of donepezil hydrochloride per day was  $26.9\pm 0.7$  or  $50.6\pm 1.9$  ng/ml (approximately 62 and 122 nM). Therefore, blocking effects of donepezil on voltage-gated ion channels in the brain are unlikely to contribute to the clinical benefits in patients with Alzheimer's disease.

## Acknowledgements

This study was supported by a grant from the National Natural Science Foundation of China (30123005).

## References

- Akasofu, S., Kosasa, T., Kimura, M., Kubota, A., 2003. Protective effect of donepezil in a primary culture of rat cortical neurons exposed to oxygen-glucose deprivation. *Eur. J. Pharmacol.* 472, 57–63.
- Cheng, D.H., Ren, H., Tang, X.C., 1996. Huperzine A, a novel promising acetylcholinesterase inhibitor. *NeuroReport* 8, 97–101.
- Choi, D.W., Rothman, S.M., 1990. The role of glutamate neurotoxicity in hypoxic–ischemic neuronal death. *Annu. Rev. Neurosci.* 13, 171–182.
- Giacobini, E., 2000. Cholinesterase inhibitors: from the Calabar bean to Alzheimer therapy. In: Giacobini, E. (Ed.), *Cholinesterases and cholinesterase inhibitors*. Martin Dunitz, London, pp. 181–226.
- Klee, R., Ficker, E., Heinemann, U., 1995. Comparison of voltage-dependent potassium currents in rat pyramidal neurons acutely isolated from hippocampal regions CA1 and CA3. *J. Neurophysiol.* 74, 1982–1995.
- Kraliz, D., Singh, S., 1997. Selective blockade of the delayed rectifier potassium current by tacrine in *Drosophila*. *J. Neurobiol.* 32, 1–10.
- Li, Y., Hu, G.-Y., 2002a. Huperzine A, a nootropic agent, inhibits fast transient potassium current in rat dissociated hippocampal neurons. *Neurosci. Lett.* 324, 25–28.
- Li, Y., Hu, G.-Y., 2002b. Huperzine A inhibits the sustained potassium current in rat dissociated hippocampal neurons. *Neurosci. Lett.* 329, 153–156.
- Palmer, A.M., 2002. Pharmacotherapy for Alzheimer's disease: progress and prospects. *Trends Pharmacol. Sci.* 23, 426–433.
- Pan, Y.-P., Xu, X.-H., Wang, X.-L., 2003. Galantamine blocks delayed rectifier, but not transient outward potassium current in rat dissociated hippocampal pyramidal neurons. *Neurosci. Lett.* 336, 37–40.
- Pan, Y.-P., Xu, X.-H., Wang, X.-L., 2004. Rivastigmine blocks voltage-activated  $\text{K}^+$  currents in dissociated rat hippocampal neurons. *Br. J. Pharmacol.* 140, 907–912.
- Raley-Susman, K.M., Kass, I.S., Cottrell, J.E., Newman, R.B., Chambers, G., Wang, J., 2001. Sodium influx blockade and hypoxic damage to CA1 pyramidal neurons in rat hippocampal slices. *J. Neurophysiol.* 86, 2715–2726.
- Rogawski, M.A., 1987. Tetrahydroaminoacridine blocks voltage-dependent ion channels in hippocampal neurons. *Eur. J. Pharmacol.* 142, 169–172.
- Rogers, S.L., Doody, R.S., Mohs, R.C., Friedhoff, L.T., the Donepezil Study Group, 1998. Donepezil improves cognition and global function in Alzheimer disease: a 15-week, double-blind, placebo-controlled study. *Arch. Intern. Med.* 158, 1021–1031.
- Sugimoto, H., Yamanishi, Y., Iimura, Y., Kawakami, Y., 2000. Donepezil hydrochloride (E2020) and other acetylcholinesterase inhibitors. *Curr. Med. Chem.* 7, 303–339.
- Takada, Y., Yonezawa, A., Kume, T., Katsuki, H., Kaneko, S., Sugimoto, H., Akaike, A., 2003. Nicotinic acetylcholine receptor-mediated neuroprotection by donepezil against glutamate neurotoxicity in rat cortical neurons. *J. Pharmacol. Exp. Ther.* 306, 772–777.
- Wang, X.-D., Chen, X.-Q., Yang, H.-H., Hu, G.-Y., 1999. Comparison of the effects of cholinesterase inhibitors on [ $^3\text{H}$ ]MK-801 binding in rat cerebral cortex. *Neurosci. Lett.* 272, 21–24.
- Zhong, C., Zhang, W., Wang, X., 2002. Effects of donepezil on the delayed rectifier-like potassium current in pyramidal neurons of rat hippocampus and neocortex. *Acta Pharm. Sin.* 37, 415–418.
- Zhou, J., Fu, Y., Tang, X.C., 2001. Huperzine A and donepezil protect rat pheochromocytoma cells against oxygen-glucose deprivation. *Neurosci. Lett.* 306, 53–56.